Transfer to Distant Retrograde Orbits via Rideshare to Sun-Earth L_1 Point

Khashayar Parsay[1] and David C. Folta[2]
NASA Goddard Space Flight Center, 8800 Greenbelt Road, Greenbelt, MD, 20771, USA

I. Introduction

Distant retrograde orbits (DRO), often classified as the f-family in the literature, are stable periodic orbits around the secondary body in the circular restricted three-body problem (CRTBP) [1, 2]. DROs are feasible for several astrophysical applications, including space telescope, space weather network, and planetary protection due to their semi-major and semi-minor axes residing beyond the L_1 and L_2 points [3, 4]. In addition to investigating the properties of Sun-Earth DROs, several studies explore the available transfer options to these unique orbits using both high-thrust and low-thrust propulsion systems [5–9]. In the case of transfers from a Low-Earth Orbit (LEO) to a Sun-Earth DRO using two impulsive maneuvers, *classical transfers*, discovered by Ocampo and Rosborough [5, 6], utilize horizontal Lyapunov orbits to construct trajectories that intersect with DROs tangentially on the x-axis of the synodic frame of the Sun-Earth system. Demeyer and Gurfil exploit manifold theory to extend the two-impulse solution space to a wider range of DRO sizes while improving the Δv cost and travel times of classical transfers [7]. Scott and Spencer further improve these studies by classifying and discovering five families of LEO-to-DRO transfers given a range of LEO altitudes and DRO sizes [8]. In addition to these notable works, several authors investigate the dynamics of DROs and the available transfer options to these orbits in the Moon-Earth system [10–13].

The main goal of this Note is to fill a small gap in the literature by quantifying the cost of

---

[1] Aerospace Engineer for Navigation and Mission Design Branch (Code 595)
[2] Senior Aerospace Engineer for Navigation and Mission Design Branch (Code 595)

transfers to Sun-Earth DROs when spacecraft are launched as a secondary payload with a primary spacecraft going to the L_1 point. This study is motivated by a few mission proposals for the NASA Small Explorers (SMEX) mission class that use DROs and require rideshare in order to cut dedicated launch services costs. First, the effects of perturbations on the size, shape, and period of Sun-Earth DROs are studied and compared to the CRTBP solutions. The transfer problem to the DRO family, via a rideshare to the Sun-Earth L_1 point, is explored next. Assuming a typical post-launch characteristic energy required to reach the L_1 point, the associated cost to establish several DROs with varying sizes are determined using a high-fidelity simulation that employs a complete ephemeris model. It is determined that the Δv cost to achieve a DRO is well within the capability of a small explorer.

II. Effects of Perturbations on DROs

Although the effects of perturbations on the size, shape, and orbital period of the DROs are small, they should be evaluated and taken into account when selecting a DRO for a mission. To quantify these effects, two sets of DRO families are computed via a differential corrector, one using the CRTBP model and one using the ephemeris model. The elliptical DROs considered have semi-minor axes (denoted by b) ranging from 2.0×10^6 km to 3.5×10^6 km, which are feasible for many deep space applications. For a given initial position in the rotating synodic frame ${}^{\mathcal{O}}\boldsymbol{r}_0 = [x_0 \;\; y_0 \;\; z_0]^T = [x_0 \;\; 0 \;\; 0]^T$, the differential corrector solves for the corresponding $\dot{y}_0$ such that the perpendicular initial velocity vector ${}^{\mathcal{O}}\dot{\boldsymbol{r}}_0 = [\dot{x}_0 \;\; \dot{y}_0 \;\; \dot{z}_0]^T = [0 \;\; \dot{y}_0 \;\; 0]^T$ leads to a trajectory that crosses the x-axis twice, achieving a bounded orbit; the algorithm searches for the required value of $\dot{y}_0$ satisfying the constraint $\dot{x} = 0$ at the second x-crossing (after one orbit). The synodic frame $\mathcal{O}$ is defined as $\mathcal{O} = \{o, \hat{\boldsymbol{e}}_x, \hat{\boldsymbol{e}}_y, \hat{\boldsymbol{e}}_z\}$, where the origin o is shifted to the secondary body (Earth), $\hat{\boldsymbol{e}}_x$ points from the Sun to the Earth, $\hat{\boldsymbol{e}}_z$ is along the ecliptic normal, and $\hat{\boldsymbol{e}}_y$ completes the right-handed coordinate system. By employing an iterative *natural parameter continuation* method, the entire family of DRO is determined. In this method, the solution of a DRO with semi-minor axis (x-crossing) of $b = x_0$, and velocity y-component, $\dot{y}_0$, is used as an initial guess to solve for the corresponding velocity y-component, $\dot{y}_0 + \Delta\dot{y}$, to the next DRO having a semi-minor axis of $b = x_0 + \Delta x$. The Δx is set to

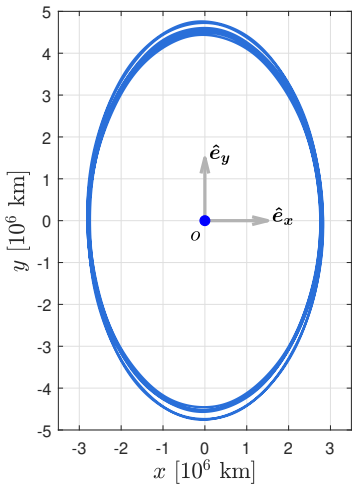

(a) DRO Propagated for Five Years

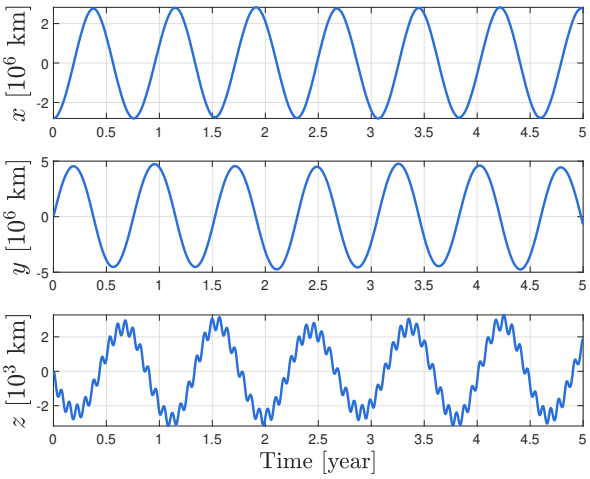

(b) DRO Position History

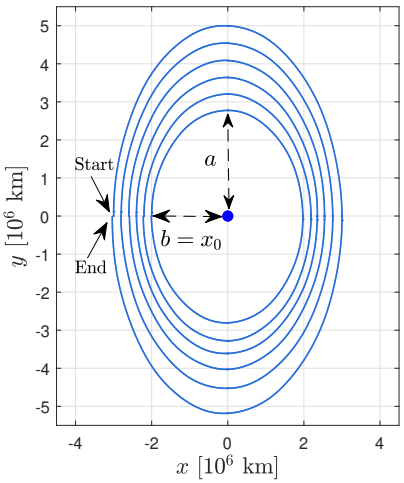

(c) A Few Members of the DRO Family

Fig. 1 DROs Computed and Propagated in Ephemeris Model

10^4 km in this study. For the second set, the General Mission Analysis Tool's (GMAT) high-fidelity force model is employed to solve for the DRO family, which includes the effects of the Earth's nonsphericity (20×20 in degree and order), solar radiation pressure (SRP), and the perturbing accelerations of the moon and all the planets in the solar system. The small spacecraft is assumed to have a total mass of 123 kg, including 23 kg of propellant, and SRP area of 0.54 m^2. Table 1 in the Appendix provides a few initial conditions computed using the method described for a randomly chosen epoch.

An example of the computed DRO in the ephemeris model is illustrated in Fig. 1(a) for the semi-minor axis of $x_0 = -2.8 \times 10^6$ km. The orbit is propagated for five years. Despite the inclusion

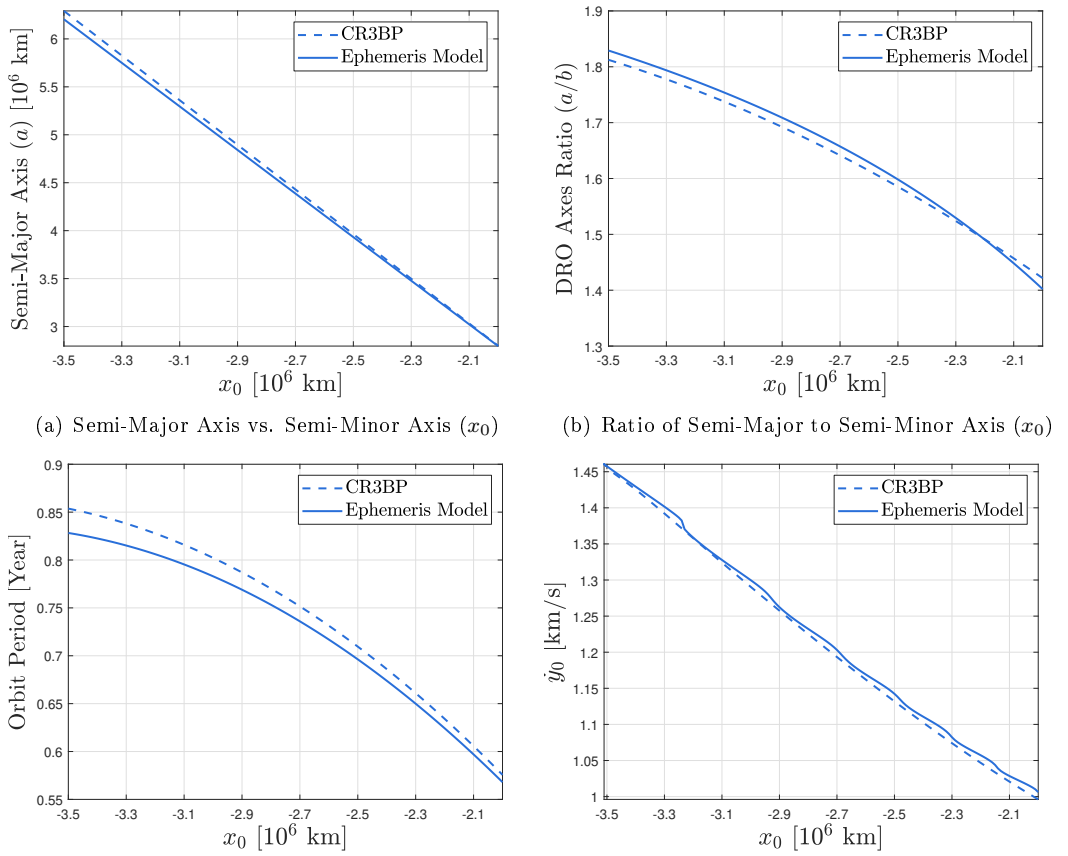

(a) Semi-Major Axis vs. Semi-Minor Axis (x_0)

(b) Ratio of Semi-Major to Semi-Minor Axis (x_0)

(c) DRO Orbit Period vs. Semi-Minor Axis (x_0)

(d) Velocity y-Component vs. Semi-Minor Axis (x_0)

Fig. 2 Effects of Perturbations on DROs' Size, Shape, and Orbit Period

of all perturbations, it is evident that the orbit is Lyapunov stable. Fig. 1(b) shows the time history of the trajectory's position components over time. Unlike the CRTBP solution, the out-of-plane component of the trajectory (z-component) propagated in the ephemeris model experiences small, but noticeable, periodic variations relative to the in-plane variations. A few other members of the DRO family are illustrated in Fig. 1(c).

The effects of perturbations on orbit size, shape, and period are illustrated in Fig. 2. As shown in Fig. 2(a), the orbit semi-major axis has a slightly smaller amplitude in the ephemeris model than in the CRTBP. The ratio of the semi-major and semi-minor axes is illustrated in Fig. 2(b). The axes ratio is higher for the orbits in the ephemeris model than that of those in the CRTBP model. Figure 2(c) demonstrates that the DROs computed in the ephemeris model have a shorter period than the ones generated in the CRTBP model. The DRO period approaches the period of the secondary body as the orbit size increases due to the perturbation effects of the secondary body gradually

diminishing. Another notable difference between the two models is the computed y-component of the initial velocity shown in Fig. 2(d). For an identical semi-minor axis of x_0, the corresponding $\dot{y}_0$ computed in the ephemeris model yields a slightly higher value. Figure 2 may be utilized by mission designers for selecting a science orbit that is compatible with their mission requirements in terms of orbit size and period.

III. Transfer Trajectory Design

In this section, the transfer problem to achieve a DRO of a particular size is studied, assuming that a spacecraft is launched as a secondary payload towards the Sun-Earth L_1 point. The initial condition considered is the post-separation state of the Deep Space Climate Observatory (DSCOVR) mission that achieved a characteristic energy of $C_3 = -0.66$ km^2/s^2. An example of a future launch opportunity to L_1 as a secondary payload is the launch of NASA's Interstellar Mapping and Acceleration Probe (IMAP) on 2024 to the Sun-Earth Lissajous orbit [14]. According to IMAP's secondary payload system interface specifications, a C_3 value between -0.68 km^2/s^2 to -0.48 km^2/s^2 is feasible and within the range of this launch opportunity. Note that the declination and right ascension launch directions are determined by the primary spacecraft (e.g. IMAP) and the secondary payload's exact orbit insertion is dependent on the excess capability of the launch vehicle after inserting the primary spacecraft.

Upon launch vehicle separation, four maneuvers are executed to achieve the desired DRO of a particular size, where each maneuver satisfies a particular constraint for the transfer trajectory. A Sequential Quadratic Programming (SQP) optimizer is employed to enforce the desired constraints and to minimize the total Δv cost, $\Delta v = \sum_{i=1}^{4} \Delta v_i$, for the transfer trajectory. The first maneuver takes place at the ecliptic crossing 48 days after separation and adjusts the orbit plane to lie on the ecliptic plane by nullifying $\dot{z}$. The second maneuver, performed two days later, targets a particular Earth flyby periapsis range. The third maneuver is performed at the orbit periapsis, and combined with the second maneuver, help with achieving the desired x-axis crossing. The fourth maneuver is performed at the arrived x-crossing to insert the spacecraft into the desired DRO, which nullifies the $\dot{x}$ and $\dot{z}$ while matching the DRO's required $\dot{y}$. To minimize the fourth maneuver, the spacecraft's

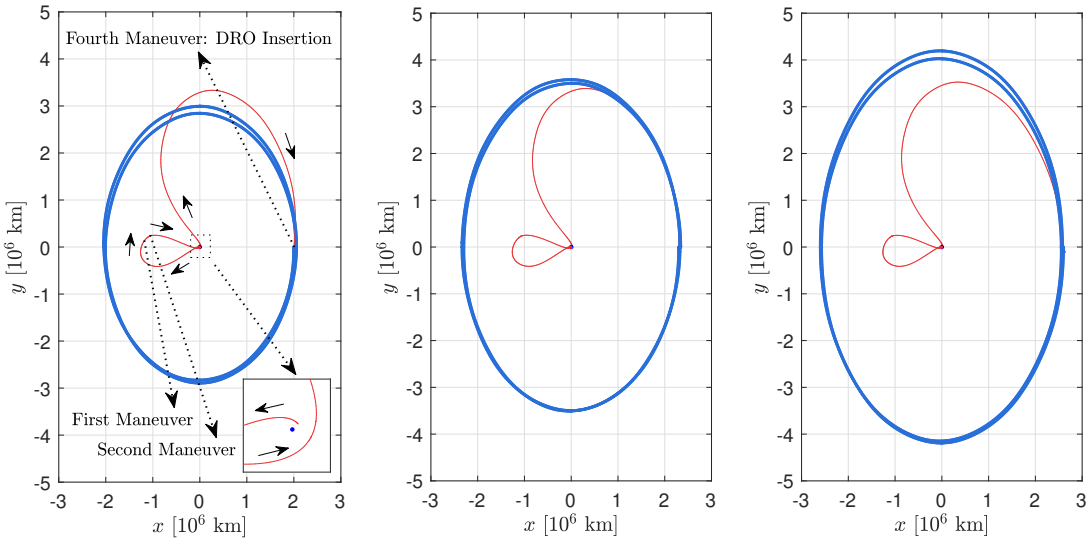

Fig. 3 Transfer to DRO of Varying Sizes from the Same Initial Condition

arrival should be perpendicular to the x-axis (i.e. $\dot{x} = \dot{z} = 0$). But given the spacecraft energy, this is achieved for only a subset of DROs. A few transfer trajectories achieving DROs with different sizes are illustrated in Fig. 3 for x-crossings of 2.0×10^6 km, 2.3×10^6 km, and 2.6×10^6 km. In each case, the achieved DRO is propagated for two orbits. The corresponding total Δv values are 361 m/s, 325 m/s, and 340 m/s, respectively. Depending on the desired size of the DRO, determined by the semi-minor axis (x-axis crossing), the transfer trajectory may or may not arrive perpendicular to the x-axis, which increases the cost of the fourth maneuver, and consequently the total Δv. On average the first, second, and third maneuvers cost about 62 m/s, 86 m/s, and 52 m/s, respectively with small variations with respect to the mean values. The fourth maneuver to insert into a DRO ranges from 122 m/s to 375 m/s, depending on the selected orbit size. The total Δv cost as a function of the arrival x-crossing is shown in Fig. 4. It is illustrated that, to achieve a DRO with a semi-minor axis between 1.7×10^6 km and 3.5×10^6 km, the total Δv cost lies between 325 m/s and 580 m/s, depending on the exact size of the desired DRO. More importantly, a certain range of the DRO family is more optimal to achieve than the rest. In this case, the DRO with the least required Δv is the one with an arrival x-crossing of 2.3×10^6 km. The travel time for the transfer trajectory ranges from 201 to 209 days.

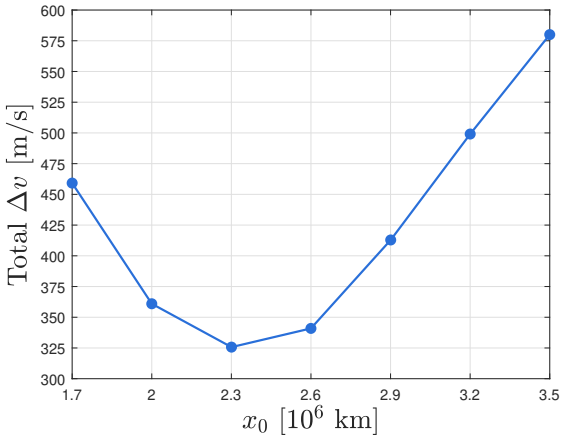

Fig. 4 Total Δv Cost for each Transfer vs. Arrival Point along x-Crossing (Semi-Minor Axis)

IV. Conclusion

In this Note, the effects of perturbations on the properties of the Sun-Earth DRO family is studied. It is shown that, given an identical semi-minor axis (x-crossing) of x_0, distant retrograde orbits have a slightly smaller amplitude, shorter period, and higher $\dot{y}_0$ value when computed in the ephemeris model than in the CRTBP model. Assuming a spacecraft is launched as a secondary payload with a primary spacecraft heading towards the L_1 point (a characteristic energy of $C_3 = -0.66$ km^2/s^2), the feasibility of designing transfer trajectories to distant retrograde orbits, whose semi-minor axes are between 1.7×10^6 km and 3.5×10^6 km, is investigated. It is determined that these orbits are achievable for small explorers and the total Δv required lies between 325 m/s to 580 m/s, depending on the orbit size.

APPENDIX A: INITIAL CONDITIONS FOR SUN-EARTH DROS

Table 1 Computed DRO Family at Randomly Chosen Epoch of Sep 1, 2026, 00:00:00.000

x_0 [10^6 km]	$\dot{y}_0$ [km/s] (CRTBP)	$\dot{y}_0$ [km/s] (Ephemeris Model)
-2.0	0.9961269668524764	1.006563566369917
-2.1	1.020718475326515	1.029521519400737
-2.2	1.046738931764639	1.058233836460361
-2.3	1.074026395752558	1.082930487923316
-2.4	1.102440829433569	1.111689301576197
-2.5	1.131875421897347	1.14319728194309
-2.6	1.162177068116719	1.170221768370744
-2.7	1.193294223106188	1.204005383272236
-2.8	1.225089811559493	1.233325012519565
-2.9	1.257541986465748	1.263323059019325
-3.0	1.290547213814055	1.300956133902025

REFERENCES

[1] Hénon, M., "Numerical exploration of the restricted problem, V," *Astronomy and Astrophysics*, Vol. 1, 1969, pp. 223–238.

[2] Hénon, M., "Numerical exploration of the restricted problem. VI. Hill's case: Non-periodic orbits." *Astronomy and Astrophysics*, Vol. 9, 1970, pp. 24–36.

[3] Stramacchia, M., Colombo, C., and Bernelli-Zazzera, F., "Distant retrograde orbits for space-based near earth objects detection," *Advances in Space Research*, Vol. 58, No. 6, 2016, pp. 967–988.

[4] Perozzi, E., Ceccaroni, M., Valsecchi, G. B., and Rossi, A., "Distant retrograde orbits and the asteroid hazard," *The European Physical Journal Plus*, Vol. 132, No. 8, 2017, p. 367.

[5] Ocampo, C. A. and Rosborough, G. W., "Transfer trajectories for distant retrograde orbiters of the Earth," *STIA*, Vol. 95, 1993, pp. 1323–1337.

[6] Ocampo, C., "Trajectory optimization for distant earth satellites and satellite constellations." .

[7] Demeyer, J. and Gurfil, P., "Transfer to distant retrograde orbits using manifold theory," *Journal of Guidance, Control, and Dynamics*, Vol. 30, No. 5, 2007, pp. 1261–1267.

[8] Scott, C. J. and Spencer, D. B., "Calculating transfer families to periodic distant retrograde orbits using differential correction," *Journal of guidance, control, and dynamics*, Vol. 33, No. 5, 2010, pp. 1592–1605.

[9] Colombo, C., Mingotti, G., Bernelli-Zazzara, F., and McInnes, C., "Multiple-spacecraft transfers to Sun-Earth distant retrograde orbits for asteroid detection missions," in "65th International Astronautical Congress (IAC 2014)," , 2014, pp. IAC–14.

[10] Ming, X. and Shijie, X., "Exploration of distant retrograde orbits around Moon," *Acta Astronautica*, Vol. 65, No. 5-6, 2009, pp. 853–860.

[11] Bezrouk, C. and Parker, J. S., "Long term evolution of distant retrograde orbits in the Earth-Moon system," *Astrophysics and Space Science*, Vol. 362, No. 9, 2017, pp. 1–11.

[12] Minghu, T., Ke, Z., Meibo, L., and Chao, X., "Transfer to long term distant retrograde orbits around the Moon," *Acta Astronautica*, Vol. 98, 2014, pp. 50–63.

[13] Capdevila, L., Guzzetti, D., and Howell, K. C., "Various transfer options from Earth into distant retrograde orbits in the vicinity of the Moon," *Earth*, Vol. 1, No. L2, 2014, p. L5.

[14] McComas, D., Christian, E. R., Schwadron, N., Fox, N., Westlake, J., Allegrini, F., Baker, D., Biesecker, D., Bzowski, M., Clark, G., et al., "Interstellar mapping and acceleration probe (IMAP): A new NASA mission," *Space science reviews*, Vol. 214, No. 8, 2018, p. 116.